

# Nonequilibrium Weak Processes in Kaon Condensation II

## — Kinetics of condensation —

Takumi Muto\*

*Department of Physics, Chiba Institute of Technology, 2-1-1 Shibazono, Narashino, Chiba  
275-0023, Japan*

Toshitaka Tatsumi†

*Department of Physics, Kyoto University, Kyoto 606-8502, Japan*

Naoki Iwamoto‡

*Department of Physics and Astronomy, The University of Toledo, Toledo, Ohio 43606-3390,  
U.S.A.*

### Abstract

The kinetics of negatively charged kaon condensation in the early stages of a newly born neutron star is considered. The thermal kaon process, in which kaons are thermally produced by nucleon-nucleon collisions, is found to be dominant throughout the equilibration process. Temporal changes of the order parameter of the condensate and the number densities of the chemical species are obtained from the rate equations, which include the thermal kaon reactions as well as the kaon-induced Urca and the modified Urca reactions. It is shown that the dynamical evolution of the condensate is characterized by three stages: the first, prior to establishment of a condensate, the second, during the growth and subsequent saturation of the condensate, and the third, near chemical equilibrium. The connection between the existence of a soft kaon mode and the instability of the noncondensed state is discussed. Implications of the nonequilibrium process on the possible delayed collapse of a protoneutron star are also mentioned.

---

\*p21mutot@cc.it-chiba.ac.jp

†tatsumi@ruby.scphys.kyoto-u.ac.jp

‡iwamoto@uoft02.utoledo.edu

## I. INTRODUCTION

The possibility that baryonic matter may undergo a transition to a new hadronic phase consisting of a condensate of negatively charged kaons ( $K^-$ ) in high density matter has been extensively discussed [1–6]. The kaon condensation may be formulated on the basis of  $SU(3)_L \times SU(3)_R$  current algebra and PCAC in a model-independent way [2,3]. Within this framework, the  $s$ -wave kaon-condensed state  $|\theta\rangle$  is generated by a chiral rotation of the normal state  $|\text{normal}\rangle$  as  $|\theta\rangle = \hat{U}_K |\text{normal}\rangle$ , where  $\hat{U}_K = \exp(i\mu_K t \hat{Q}) \exp(i\theta \hat{Q}_4^5)$  is a unitary operator. Here  $\mu_K$  is the kaon chemical potential,  $\theta$  the chiral angle, which is the order parameter of the condensate, and  $\hat{Q}$  ( $\hat{Q}_4^5$ ) is the electromagnetic charge operator (the axial charge operator). The classical  $K^-$  field is then written as  $\langle K^- \rangle \equiv \langle \theta | K^- | \theta \rangle = (f/\sqrt{2}) \sin \theta \exp(-i\mu_K t)$  with  $f (=93 \text{ MeV})$  the meson decay constant.

Kaon condensation is a form of Bose-Einstein condensation (BEC): the lowest excitation energy of the  $K^-$  decreases in a nuclear medium with an increase in the baryon number density due to an attractive  $s$ -wave kaon-nucleon ( $KN$ ) interaction. When the lowest excitation energy becomes equal to the charge chemical potential, the distribution function for the  $K^-$  diverges and a macroscopic number of kaons appear. The relevant  $s$ -wave  $KN$  interaction comes mainly from the scalar interaction (the  $KN$  sigma term,  $\Sigma_{KN}$ ) and the vector interaction (the Tomozawa-Weinberg term) [2–4].

The baryon number density for the onset of kaon condensation in stable neutron-star matter has been predicted to be 3–4 times the nuclear matter density  $n_0$  ( $=0.16 \text{ fm}^{-3}$ ), depending on the magnitude of  $\Sigma_{KN}$ . Motivated by studies of kaon condensation, the in-medium  $KN$  interaction has recently been elaborated both theoretically and experimentally, through  $KN$  scattering [7–9], kaonic atoms [10], and kaon-antikaon production via relativistic nucleus-nucleus collisions [11–15]. The experimental results suggest a substantial decrease in the antikaon effective mass, which in turn favors the possible existence of a kaon condensate in the core of a neutron star.

The appearance of the kaon-condensed phase in a neutron star would lead to softening of the equation of state (EOS) [3,12,16] and also accelerate cooling of neutron stars [16–20]. The softening of the EOS associated with kaon condensation has been used to construct a model in which the collapse of a hot protoneutron star to a black hole is delayed [21–23]<sup>1</sup>; initially, there is no kaon condensation in protoneutron stars, since the neutrino degeneracy and thermal effects raise the threshold density for kaon condensation. A kaon condensate is formed during the evolution into a compact neutron star through deleptonization and cooling. The maximum mass of the kaon-condensed neutron star is estimated to be  $\sim 1.5 M_\odot$  with  $M_\odot$  the solar mass [3,12,16], which is smaller than the maximum mass of ordinary neutron stars ( $\sim 2.0 M_\odot$ ) [29] because of the significant softening of the EOS due to the appearance of the condensates. If the mass of a protoneutron star after deleptonization or cooling exceeds the maximum mass of the kaon-condensed neutron star, the star eventually collapses to a black hole. Such a scenario for the formation of a low-mass black hole ( $1.5\text{--}2.0 M_\odot$ ) has been presented by Brown and Bethe [21] to interpret the absence of a pulsar signature in SN 1987A [30]. Following their scenario,

---

<sup>1</sup>Similar delayed collapse mechanisms of a hot protoneutron star to a more compact neutron star or to a black hole, attributed to other hadronic phase transitions, have been considered by some authors [5,24–28].

Baumgarte et al. made a numerical simulation for the delayed collapse of a protoneutron star by the use of an EOS including the phase transition to the kaon-condensed phase [22].

In these studies, the equilibrated EOS with kaon condensation was used. The kaons are created through *weak interactions* that change strangeness during the appearance and the growth of the condensate, and the time scale for the weak reactions are much larger than those for the strong and electromagnetic reactions which are responsible for the thermal equilibration of the system. In addition, there are at least three time scales which characterize the dynamical evolution of a newly born neutron star: the time scale for gravitational collapse (of order of a millisecond) and those for deleptonization and initial cooling (of order of a second and ten seconds, respectively). If the weak reactions which are responsible for the formation of a condensate proceed on a longer time scale than these time scales, they may control the dynamical evolution of a neutron star just after a supernova explosion. In this case, the nonequilibrium processes in kaon condensation which are brought about by the weak reactions must be considered.

The time evolution of the system is determined by the Hamiltonian,

$$\hat{H} = \hat{H}_{\text{strong}} + \hat{H}_{\text{weak}} , \quad (1)$$

with the strong (weak) Hamiltonian  $\hat{H}_{\text{strong}}$  ( $\hat{H}_{\text{weak}}$ ). In our case the state  $|\theta(t), t\rangle$  is specified by the parameters,  $\theta$ ,  $\mu_n$  ( $\mu_p$ ) the neutron chemical potential (the proton chemical potential),  $\mu_K$ , and  $\mu_e$  the electron chemical potential, for given temperature  $T$  and baryon number density  $n_B$ . Alternatively we may choose another set of operators,  $\hat{\theta}$ , the number densities  $\hat{n}_i$  ( $i = p, n, K, e$ ) to specify the state. If the weak Hamiltonian  $\hat{H}_{\text{weak}}$  is negligibly small, then the time scale of the weak interaction is very large ( $\tau_{\text{weak}} \gg \tau_{\text{strong}}$ ). In such a case, it is obvious that all the number densities are time-independent,  $\dot{\hat{n}}_i=0$ , which in turn implies  $\dot{\hat{\theta}}=0$ , or they can commute with  $\hat{H}_{\text{strong}}$ ,  $[\hat{n}_i, \hat{H}_{\text{strong}}]=0$ , due to baryon number, strangeness, charge and lepton number conservations. Thus we can find the simultaneous eigenstate of  $\hat{H}_{\text{strong}}$  and  $\hat{n}_i$ . Hence, if we apply the adiabatic (Born-Oppenheimer) approximation, then the time-dependence of  $n_i(t) \equiv \langle \theta(t), t | \hat{n}_i | \theta(t), t \rangle$  is determined by the weak interaction Hamiltonian  $\hat{H}_{\text{weak}}$ , which leads to the rate equations. With  $n_i(t)$  taken to be a function of time, it is possible to fix the time and construct an instantaneous eigenstate of  $\hat{H}_{\text{strong}}$  and  $\hat{\theta}$ , by considering the extremum conditions for the thermodynamic potential  $\Omega$  given only by the strong interaction Hamiltonian  $\hat{H}_{\text{strong}}$ ,

$$|\theta(t), t\rangle \simeq |\theta(t), n_K(t), n_n(t), n_p(t), n_e(t)\rangle. \quad (2)$$

Solving the rate equations then allows the temporal change of  $n_i$  to be determined, while the time dependence of the order parameter  $\theta$  is determined by use of the thermodynamic potential  $\Omega$ .

The nonequilibrium processes in the kaon-condensed state  $|\theta(t), t\rangle$  have been previously investigated in [31], with account taken of both the kaon-induced Urca process and the modified Urca process. The former process (abbreviated to KU-F and KU-B, where F and B stand for forward and backward reactions, respectively) is represented by the reactions

$$n(p) \rightarrow n(p) + e^- + \bar{\nu}_e, \quad (3a)$$

$$n(p) + e^- \rightarrow n(p) + \nu_e , \quad (3b)$$

and provides the most efficient cooling mechanism for the star via neutrino and antineutrino emissions [17,18]. In terms of the condensate  $\langle K^- \rangle$ , by which the system is supplied with energy and the reactions become kinematically possible, the KU process (3) can be written symbolically as  $n(p) + \langle K^- \rangle \rightarrow n(p) + e^- + \bar{\nu}_e$ ,  $n(p) + e^- \rightarrow n(p) + \langle K^- \rangle + \nu_e$ . The modified Urca process (MU-F and MU-B) [32,33], represented by the reactions

$$n + n \rightarrow n + p + e^- + \bar{\nu}_e, \quad (4a)$$

$$n + p + e^- \rightarrow n + n + \nu_e, \quad (4b)$$

is a standard cooling process for a normal neutron star.<sup>2</sup> Because the transition matrix element for KU is proportional to  $\sin \theta$ , this process is operative only in the presence of a condensate. Thus, spontaneous creation of a condensate from the noncondensed state cannot occur solely by way of the KU and MU reactions, and, for this reason in Ref. [31], a small seed of the condensate ( $\theta \neq 0$ ) was put in by hand.

In the noncondensed state, kaons are produced thermally by the weak reactions

$$n + n \rightarrow n + p + K^-, \quad (5a)$$

$$n + p + K^- \rightarrow n + n, \quad (5b)$$

where a spectator neutron must take part in the reactions such that the kinematical condition in a degenerate Fermi system is satisfied. The thermal kaons are then converted to a condensate. Thus we can discuss the onset and the growth of a kaon condensate consistently without any ad hoc seed (see Sec.III), in which case the process (5) is primarily responsible for the onset of condensation. We will refer to the reaction (5) as the thermal kaon process, and abbreviate them to KT-F and KT-B, respectively.

In a previous paper [37] (Paper I), we have obtained the reaction rate for KT, and discussed the effects of thermal kaons on the KT reaction rate in both the noncondensed and condensed states. We have also compared the KT reaction rate with the rates for the KU and MU reactions and obtained the following results: (i) In the noncondensed state, where the system is far from chemical equilibrium, hard thermal kaons with large momenta make the major contribution to the KT reaction rate, whereas in the condensed state, the soft thermal kaons, which appear as a Goldstone mode from the spontaneous breaking of  $V$ -spin symmetry, contribute significantly to the KT reaction rate. (ii) The KT reaction rate is larger than the rates for the KU and MU reactions over the relevant temperatures and baryon number densities. (iii) The KT process is dominant in the kaon-condensed state in chemical equilibrium as well as in the noncondensed state, and may determine the evolution of the system.

Based on the above results for the KT reactions, we in this paper, investigate the nonequilibrium weak processes in kaon condensation by taking into account the KT process as well as the KU and MU processes, and clarify the effects of thermal kaons on the kinetics of condensation. Assuming that the system is in thermal equilibrium, we solve the rate equations given by the relevant weak reactions (3)–(5), and discuss the temporal behavior of the number densities of the chemical species, the order parameter of the

---

<sup>2</sup> Throughout this paper, we do not take into account the direct Urca process in the normal phase [34,35] or in the kaon-condensed phase [16,20], and also omit other weak reactions associated with hyperons [36], taking the same standpoint as in Paper I.

condensate, and other physical quantities. In general, the energy, produced in the course of the nonequilibrium process, is dissipated into the surroundings, resulting in a rise in the temperature of the system. For simplicity, however, the temperature is kept constant throughout this paper. We find two characteristic time scales for the onset of a condensate and its subsequent growth. The magnitudes of these time scales are compared with other time scales characterizing the collapse of a newly-born neutron star, and possible effects on stellar collapse are discussed.

The paper is organized as follows: The description of the nonequilibrium state based on the thermodynamic potential is addressed in Sec. II, and the formulation for obtaining the rate equations is given in Sec. III. The numerical results are then presented in Sec. IV, and summary and concluding remarks are given in Sec. V. In Appendix A, an asymptotic behavior of the system near chemical equilibrium is discussed. Specifically, an expression for the relaxation time near chemical equilibrium is derived analytically.

## II. DESCRIPTION OF THE NONEQUILIBRIUM STATE

### A. Thermodynamic potential

Here we define the physical conditions for a nonequilibrium kaon-condensed state,  $|\theta(t), t\rangle$ .<sup>3</sup> The system is described by a thermodynamic potential  $\Omega$ . The microscopic quantities, such as the excitation energies of the baryons and the thermal and condensed kaons, are determined by the strong and electromagnetic interactions among the kaons, baryons and leptons. The time scales for these interactions are much smaller than those for weak reactions. Therefore, in setting up the kinetic equations, that determine the relatively slow change of chemical composition via weak reactions, the system may be assumed to be in thermal equilibrium, maintained by much faster strong and electromagnetic reactions. As a consequence, the physical quantities for the nonequilibrium state evolve adiabatically, adjusting to the gradual change of the chemical composition brought about by the weak processes.

Assuming thermal equilibrium, we adopt the thermodynamic potential  $\Omega$  of the kaon-condensed phase which was derived by Tatsumi and Yasuhira from chiral symmetry [38], including the thermal and quantum fluctuations around a condensate. In the present work, we shall neglect, for the sake of simplicity, both zero-point and thermal fluctuations in the thermodynamic variables except for the thermal contribution to the kaon number density, which allows us to see the effects of thermal kaons on the kinetics of condensation. Thus our expression for  $\Omega$  corresponds to the heavy-baryon limit for the nucleons [38]. With these assumptions, the thermodynamic potential per unit volume  $\Omega/V$  of the kaon-condensed phase is written as

$$\Omega/V = (\Omega_C + \Omega_K + \Omega_N + \Omega_e)/V , \quad (6)$$

where  $\Omega_C$  and  $\Omega_K$  are the potentials arising from a condensate and thermal fluctuations for the kaons, respectively, and  $\Omega_N$  and  $\Omega_e$  are the corresponding potentials for the nucleons and the electrons, respectively. Here,  $\Omega$ , the number density  $n_i$  and the chemical potential

---

<sup>3</sup> We use the units in which  $\hbar=c=k_B=1$  throughout this paper.

$\mu_i$  ( $i = p, n, e^-, K$ ) are related to each other by  $n_i = -\partial(\Omega/V)/\partial\mu_i$ . Specifically, the classical contribution from the condensate,  $\Omega_C$ , is given by

$$\Omega_C/V = f^2 m_K^2 (1 - \cos \theta) - \frac{1}{2} f^2 \mu_K^2 \sin^2 \theta, \quad (7)$$

where  $m_K$  is the free kaon mass ( $= 494$  MeV). In contrast, the thermal kaon contribution,  $\Omega_K$ , is given by

$$\Omega_K/V = T \int \frac{d^3 p_K}{(2\pi)^3} \ln \left( 1 - e^{-[\omega_+(\mathbf{p}_K) + \mu_K]/T} \right) \left( 1 - e^{-[\omega_-(\mathbf{p}_K) - \mu_K]/T} \right), \quad (8)$$

with  $\omega_+(\mathbf{p}_K)$  [ $\omega_-(\mathbf{p}_K)$ ] the excitation energy for  $K^+$  ( $K^-$ ) (cf. Sec. II B for the explicit expressions for  $\omega_\pm(\mathbf{p}_K)$ ), and the nucleon contribution  $\Omega_N$  is written in the standard form:

$$\Omega_N/V = \mathcal{E}_N - \mu_p n_p - \mu_n n_n \quad (9)$$

where the energy density for the nucleons is given by

$$\mathcal{E}_N = \frac{3}{5} \frac{(3\pi^2)^{2/3}}{2m_N} \left( n_p^{5/3} + n_n^{5/3} \right) - f^2 (\sigma + 2b\mu_K) (1 - \cos \theta) + V_{\text{sym}}(n_B) (n_p - n_n)^2 / n_B. \quad (10)$$

The first term in the r.h.s. of Eq. (10) is the nucleon Fermi-gas energy density, with  $m_N$  the nucleon mass, and the quantity  $\sigma$  in the second term defined as  $\sigma \equiv n_B \Sigma_{KN} / f^2$ , and  $b \equiv (n_p + \frac{1}{2} n_n) / (2f^2)$  is the  $V$ -spin density [see Sec. IV A for specific values]. The terms involving  $\sigma$  and  $b$ , respectively, come from the  $s$ -wave  $K^-N$  interaction given by the  $KN$  sigma term and the Tomozawa-Weinberg term. The expression for the energy contribution from kaon-kaon and kaon-nucleon interactions is essentially determined in a model-independent way by chiral symmetry. The third term in Eq.(10) is the potential energy contribution to the symmetry energy. For  $V_{\text{sym}}(n_B)$ , we use the expression given by Prakash et al. [39]:

$$V_{\text{sym}}(n_B) = \left[ S_0 - (2^{2/3} - 1) \frac{3}{5} \epsilon_{F,0} \right] F(n_B), \quad (11)$$

where  $S_0$  ( $= 30$  MeV) is the empirical symmetry energy, and  $\epsilon_{F,0}$  is the Fermi energy in the symmetric nuclear matter at the density  $n_0$ , with the function  $F(n_B)$  taken as  $F(n_B) = n_B/n_0$  for simplicity. The chemical potentials for the proton and the neutron, respectively, in (9) are given by  $\mu_p = \partial\mathcal{E}_N/\partial n_p$  and  $\mu_n = \partial\mathcal{E}_N/\partial n_n$ , respectively, so that the difference between  $\mu_p$  and  $\mu_n$  in the condensed state is written as

$$\begin{aligned} \mu_p - \mu_n &= \frac{(3\pi^2 n_p)^{2/3}}{2m_N} - \frac{(3\pi^2 n_n)^{2/3}}{2m_N} + 4V_{\text{sym}}(n_B) \cdot (n_p - n_n) / n_B \\ &\quad - \frac{1}{2} \mu_K (1 - \cos \theta). \end{aligned} \quad (12)$$

For  $\Omega_e$ , we use the ultrarelativistic form for electrons,

$$\Omega_e/V = \frac{\mu_e^4}{4\pi^2} - \mu_e n_e = -\frac{\mu_e^4}{12\pi^2}, \quad (13)$$

where  $\mu_e$  is the electron chemical potential and  $n_e [= \mu_e^3 / (3\pi^2)]$  is the electron number density. Note that  $\mu_e \neq \mu_K$  when the system is not in chemical equilibrium.

## B. Thermal kaon excitation

As can be seen in Eq.(6), only the thermal kaon excitations constitute the thermal fluctuations in the thermodynamic potential  $\Omega$ , because they are responsible for the formation of a condensate through the weak reactions KT[(5)]. The excitation energy for the thermal kaons,  $\omega_{\pm}(\mathbf{p}_K)$ , appearing in  $\Omega_K$  [Eq.(8)], is obtained from the dispersion relations for kaon modes in the condensed state. The expression for  $\omega_{\pm}(\mathbf{p}_K)$  depends on the method for treating the fluctuations around the condensate [38,40], but numerical results have shown that there is little difference between the two methods used in Refs. [38] and [40]. Later on we use the result of Ref. [38]:

$$\omega_{\pm}(\mathbf{p}_K) \simeq \pm \left\{ b + \mu_K (\cos \theta - 1) \right\} + \left[ \mathbf{p}_K^2 + (b^2 + \widetilde{m}_K^{*2}) \right]^{1/2}, \quad (14)$$

where  $\widetilde{m}_K^{*2} \equiv m_K^{*2} \cos \theta = (m_K^2 - \sigma) \cos \theta$ , and  $m_K^*$  denotes the effective kaon mass which is reduced due to the  $KN$  scalar interaction  $\Sigma_{KN}$  [3]. Using (14) one obtains the total kaon number density from the relation,  $n_K = -\partial(\Omega/V)/\partial\mu_K$ :

$$n_K = \zeta_K + n_K^T. \quad (15)$$

Here  $\zeta_K$  is the condensed part of the kaon number density :

$$\begin{aligned} \zeta_K &\equiv -\partial(\Omega_C/V + \Omega_N/V)/\partial\mu_K \\ &= \mu_K f^2 \sin^2 \theta + 2bf^2(1 - \cos \theta), \end{aligned} \quad (16)$$

and  $n_K^T$  is the thermal part:

$$\begin{aligned} n_K^T &= -\partial(\Omega_K/V)/\partial\mu_K \\ &= \frac{1}{(2\pi)^3} \cos \theta \int d^3 p_K f_K(\mathbf{p}_K) \end{aligned} \quad (17)$$

with

$$f_K(\mathbf{p}_K) = \frac{1}{e^{[\omega_-(\mathbf{p}_K) - \mu_K]/T} - 1} - \frac{1}{e^{[\omega_+(\mathbf{p}_K) + \mu_K]/T} - 1}, \quad (18)$$

where the first and second terms are the Bose-Einstein distribution functions for the  $K^-$  and  $K^+$  mesons, respectively. It is to be noted that the expression (17) is slightly different from the usual one for the noncondensed state by a reduction factor  $\cos \theta$  due to the existence of the condensate. The expression (16) is equivalent to the strangeness number density  $\zeta_K = \langle K^- | \hat{S} | K^- \rangle$  with the strangeness operator  $\hat{S} \equiv 2(\hat{Q} - \hat{I}_3 - \hat{B})$ .

By the use of the classical field equation for  $\theta$ ,  $\partial\Omega/\partial\theta = 0$  [3,38],

$$\sin \theta \left( \mu_K^2 \cos \theta + 2b\mu_K - m_K^{*2} \right) = 0, \quad (19)$$

which is valid where fluctuations of kaons can be neglected [38], it can be seen from (14) that, in the condensed phase ( $\theta \neq 0$ ), the lowest excitation energy of  $K^-$  is equal to the kaon chemical potential, i.e.,  $\omega_-(\mathbf{p}_K = 0) = \mu_K$ . This soft mode results from the spontaneous  $V$ -spin symmetry breaking in the condensed phase (Goldstone mode), and leads to a divergence of  $f_K(\mathbf{p}_K)$  at  $\mathbf{p}_K=0$  in the condensed state. On the other hand,

in the limit  $\theta = 0$  in Eq.(14), one obtains the excitation energy of kaons in the normal (noncondensed) phase:

$$\omega_{\pm}(\mathbf{p}_K) = \pm b + [\mathbf{p}_K^2 + (b^2 + m_K^{*2})]^{1/2}. \quad (20)$$

In this case, there is a gap between the lowest excitation energy  $\omega_-(\mathbf{p}_K = 0)$  and  $\mu_K$ , so that  $f_K(\mathbf{p}_K)$  has no singularity. The appearance of a soft kaon mode is also related to an instability of the normal state with respect to the onset of a condensate. (See also Sec.IV A.)

### III. KINETICS OF CONDENSATION

#### A. Rate Equations

The thermally excited kaons, which are produced via the weak reactions KT, are converted into a condensate through kaon-nucleon and kaon-kaon scatterings:  $KN \rightarrow \langle K \rangle N$ ,  $KK \rightarrow K \langle K \rangle$ . The time required for the conversion of the thermal kaons to a condensate through strong interaction collisions is negligible compared with the time scale governed by the weak reactions. This is consistent with the assumption that the system is in *thermal equilibrium*, as discussed in Sec.II A. Thus, we put aside the detailed conversion mechanisms of the thermal kaons into a condensate, and study the kinetics of condensation due to the weak reactions to obtain the typical time scales for the development of a condensate. With the kaon number density given by Eq.(15), one can see that the condensate appears spontaneously once the number density of the thermal kaons is saturated for a given temperature. With this simplification, we can describe the growth of the condensate during the whole nonequilibrium stage by following the kinetics of the condensate semiclassically, avoiding the discussion of quantum nucleation of the condensates.

In general, the heat released by dissipation of energy in the system is expected to increase the temperature  $T$ . The temporal change of the temperature,  $T(t)$  can be obtained from the equation that gives the rate of change of the internal energy of the system: e.g.,

$$\partial E / \partial t = -\epsilon_{\nu} - \epsilon_{\bar{\nu}} \quad (21)$$

with  $\epsilon_{\nu}$ ,  $\epsilon_{\bar{\nu}}$  the luminosities of neutrinos and antineutrinos, respectively, for the neutrino-free-streaming case. For simplicity, however, we take the temperature to be constant during the nonequilibrium process. A more realistic calculation including the variation of the temperature will be discussed in the future.

The number density of each chemical species is determined by the rate equations, with the rates of change of the electron ( $n_e$ ), the kaon ( $n_K$ ), and the proton ( $n_p$ ) number densities given by

$$\begin{aligned} dn_e(t)/dt &= \Gamma^{(KU-F)}(\xi^{(KU)}(t), T) - \Gamma^{(KU-B)}(\xi^{(KU)}(t), T) \\ &\quad + \Gamma^{(MU-F)}(\xi^{(MU)}(t), T) - \Gamma^{(MU-B)}(\xi^{(MU)}(t), T), \end{aligned} \quad (22a)$$

$$\begin{aligned} dn_K(t)/dt &= -\Gamma^{(KU-F)}(\xi^{(KU)}(t), T) + \Gamma^{(KU-B)}(\xi^{(KU)}(t), T) \\ &\quad + \Gamma^{(KT-F)}(\xi^{(KT)}(t), T) - \Gamma^{(KT-B)}(\xi^{(KT)}(t), T), \end{aligned} \quad (22b)$$

$$dn_p(t)/dt = \Gamma^{(MU-F)}(\xi^{(MU)}(t), T) - \Gamma^{(MU-B)}(\xi^{(MU)}(t), T)$$



$$+ \Gamma^{(\text{KT-F})}(\xi^{(\text{KT})}(t), T) - \Gamma^{(\text{KT-B})}(\xi^{(\text{KT})}(t), T) , \quad (22c)$$

where  $\Gamma^{(\alpha)}$  are the reaction rates ( $\alpha = \text{KU}, \text{MU}, \text{KT}$ ), and ‘F’ (‘B’) denotes the forward (backward) process. As a consequence of baryon number conservation, the rate of change of the neutron number density is determined by  $dn_p(t)/dt$  through the equation  $dn_n(t)/dt = -dn_p(t)/dt$ .

## B. Reaction rates

Since the kaon-condensed state is obtained from the underlying chiral symmetry [37], the matrix elements for the relevant reactions can be calculated from the chirally-transformed weak Hamiltonian. The expressions for these reaction rates have been given in paper I [37]. Here we only show the results. For the forward KT process (5a), denoted as KT-F, one obtains

$$\begin{aligned} \Gamma^{(\text{KT-F})}(\xi^{(\text{KT})}, T) &= \frac{512}{9(2\pi)^7} \left( g_A G_F \tilde{f}^2 f \sin \theta_C \cos \theta_C \cos^3 \frac{\theta}{2} \frac{|\mathbf{p}_F(n)|^2}{|\mathbf{p}_F(n)|^2 + m_\pi^2} \right)^2 |\mathbf{p}_F(p)| \\ &\times (m_n^*)^3 m_p^* T^5 I^{(\text{KT})}(\xi^{(\text{KT})}, T) \end{aligned} \quad (23a)$$

$$= (4.0 \times 10^{30}) \left( \frac{|\mathbf{p}_F(p)|}{m_\pi} \right) \left( \frac{m_n^*}{m_N} \right)^3 \left( \frac{m_p^*}{m_N} \right) \cos^6 \frac{\theta}{2} T_9^5 I^{(\text{KT})}(\xi^{(\text{KT})}, T) \quad (\text{cm}^{-3} \cdot \text{s}^{-1}) , \quad (23b)$$

where  $\xi^{(\text{KT})} \equiv (\mu_K + \mu_p - \mu_n)/T$  and  $I^{(\text{KT})}(u, T)$  is the integral over the kaon momentum divided by  $T$ , with  $x = |\mathbf{p}_K|/T$ :

$$I^{(\text{KT})}(u, T) \equiv \frac{1}{6} \int_0^\infty dx \frac{x^4}{(\tilde{\omega}_-(x) + \mu_K/T)^3} \frac{(\tilde{\omega}_-(x) + u)}{1 - e^{-\tilde{\omega}_-(x)}} \frac{[(\tilde{\omega}_-(x) + u)^2 + 4\pi^2]}{e^{\tilde{\omega}_-(x)+u} - 1} \quad (24)$$

where  $\tilde{\omega}_-(x) \equiv (\omega_-(x) - \mu_K)/T$ . In (23a),  $g_A (=1.25)$  is the axial-vector coupling strength,  $\tilde{f} \equiv f_{\pi NN}/m_\pi$  the  $\pi NN$  coupling strength divided by the pion mass,  $G_F$  the Fermi coupling constant, and  $\theta_C (\simeq 0.24)$  the Cabibbo angle. The factor  $g_A G_F f \sin \theta_C \cos \theta_C \cos^3 \frac{\theta}{2}$  originates from a  $npK^-$  vertex factor in the transition matrix elements obtained from the chirally-rotated hadron currents, whereas the other factor,  $\tilde{f}^2 \frac{|\mathbf{p}_F(n)|^2}{|\mathbf{p}_F(n)|^2 + m_\pi^2}$  with  $\mathbf{p}_F(i)$  ( $i = n, p$ ) the Fermi momentum, comes from the one-pion exchange potential introduced to describe the long-range part of the interactions. Due to the approximate kinematical condition [37], only the nucleon axial-vector current (proportional to  $g_A$ ) is found to contribute to the KT reactions after all the matrix elements for the lowest-order diagrams are summed. Hence the current for the  $s$ -wave condensate, which has only a time component, does not couple to the nonrelativistic nucleon current. The remaining factor in (23a) arises from the phase space integrals in which  $m_n^*$  is the effective nucleon mass and  $T_9$ , the temperature in units of  $10^9$  K. For simplicity, we take the values of the nucleon effective masses to be  $m_p^*/m_N = m_n^*/m_N = 0.8$  [32].

For the forward KU process (KU-F) [(3a)], one obtains

$$\Gamma^{(\text{KU-F})}(\xi^{(\text{KU})}, T) = \frac{G_F^2}{64\pi^5} \sin^2 \theta_C \sin^2 \theta \left\{ 10 + 3(g_A^2 + 9\tilde{g}_A^2) \right\} m_N^{*2} \mu_e T^5 I_2(\xi^{(\text{KU})})$$

$$= (6.6 \times 10^{29}) \left( \frac{m_N^*}{m_N} \right)^2 \frac{\mu_e}{m_\pi} \sin^2 \theta(t) T_9^5 I_2(\xi^{(\text{KU})}) \text{ (cm}^{-3} \cdot \text{s}^{-1}) \quad (25)$$

where  $\tilde{g}_A = F - \frac{1}{3}D = 0.15$  with  $F + D = g_A = 1.25$ ,  $D/(D + F) = 0.658$  [20],  $I_2(u) \equiv \int_0^\infty dx x^2 [\pi^2 + (x + u)^2] / (1 + \exp(x + u))$  and  $\xi^{(\text{KU})} \equiv (\mu_e - \mu_K)/T$ . That the rate for KU-F is proportional to  $\sin^2 \theta$  is derived from the fact that the matrix element for KU-F is proportional to  $\sin \theta$ . As a consequence, the KU reactions are operative only when a condensate is present.

For the forward MU process (MU-F) [(4a)], we refer to Haensel's result [41]:

$$\Gamma^{(\text{MU-F})}(\xi^{(\text{MU})}, T) = (5.9 \times 10^{23}) \left( \frac{n_e}{n_0} \right)^{1/3} \cos^2 \frac{\theta}{2} T_9^7 J_2(\xi^{(\text{MU})}) \text{ (cm}^{-3} \cdot \text{s}^{-1}) , \quad (26)$$

where  $J_2(u) \equiv \int_0^\infty dx x^2 [9\pi^4 + 10\pi^2(x + u)^2 + (x + u)^4] / (1 + \exp(x + u))$ , and  $\xi^{(\text{MU})} \equiv (\mu_p + \mu_e - \mu_n)/T$ . Here, the matrix elements have been slightly modified by inclusion of an additional factor of  $\cos^2(\theta/2)$  due to the presence of a condensate (cf. Paper I).

The backward processes, denoted by the suffix B, are related to the forward processes by way of the following relations:

$$\Gamma^{(\text{KT-B})}(\xi^{(\text{KT})}, T) = e^{\xi^{(\text{KT})}} \Gamma^{(\text{KT-F})}(\xi^{(\text{KT})}, T) , \quad (27)$$

and

$$\Gamma^{(\text{KU-B})}(\xi^{(\text{KU})}, T) = \Gamma^{(\text{KU-F})}(-\xi^{(\text{KU})}, T) , \quad \Gamma^{(\text{MU-B})}(\xi^{(\text{MU})}, T) = \Gamma^{(\text{MU-F})}(-\xi^{(\text{MU})}, T) \quad (28)$$

which are valid at low temperatures [37]. The relation (27) between the forward and backward reaction rates for KT (where bosons are involved) differs from the corresponding relations (28) in the case of the KU or MU process (where only fermions are involved).

### C. Initial conditions

We adopt the following initial conditions: At  $t=0$ , we assume normal neutron-star matter ( $\theta = 0$ ), composed of nonrelativistic protons ( $p$ ), neutrons ( $n$ ), and ultra-relativistic free electrons ( $e^-$ ), which is charge neutral,  $n_p^0 = n_e^0$ .<sup>4</sup> The baryon number density  $n_B$  for the noncondensed state is taken to be larger than the critical density for kaon condensation,  $n_B^C (=3-4 n_0)$ . Initially, the system is assumed to be in  $\beta$ -equilibrium, i.e.,  $\mu_n^0 = \mu_p^0 + \mu_e^0$  [ $\xi^{(\text{MU})}(t=0) = 0$ ] due to the rapid  $\beta$ -decay reactions,  $n \rightarrow p + e^- + \bar{\nu}_e$ ,  $p + e^- \rightarrow n + \nu_e$ , when the neutron star is hot at an early stage. The initial values for the proton fraction  $x_p^0 \equiv n_p^0/n_B$  and for the electron chemical potential  $\mu_e^0$  are then obtained from the charge neutrality condition,  $n_B x_p^0 = (\mu_e^0)^3 / (3\pi^2)$ , and the  $\beta$ -equilibrium condition where Eq.(12) is used with  $\theta = 0$ . Finally, the total strangeness is assumed to be almost zero corresponding to equal numbers of thermal  $K^+$ 's and  $K^-$ 's present, which, using Eqs. (14), (17) and (18) with  $\theta = 0$ , gives the initial value of the kaon chemical

<sup>4</sup>The superscript '0' denotes the initial value at  $t = 0$ .

potential  $\mu_K^0 = -b^0$ . As a consequence of these conditions, the initial kaon chemical potential  $\mu_K^0$  has a large negative value, while  $\mu_e^0$  is positive. Thus the system is far from chemical equilibrium with  $|\xi^{(\text{KT})}(t=0)| = |\xi^{(\text{KU})}(t=0)| = |(\mu_e^0 - \mu_K^0)/T| \gg 1$ . For example, one obtains  $\xi^{(\text{KT})}(t=0) = -46$  and  $\xi^{(\text{KU})}(t=0) = 46$  for  $\Sigma_{KN} = 300$  MeV,  $n_B = 0.55 \text{ fm}^{-3}$  and  $T = 1 \times 10^{11} \text{ K}$ . Starting from these initial conditions, one can first obtain the number densities  $n_i(t)$  at later times from the rate equations (22). Next one can obtain the electron chemical potential  $\mu_e(t)$  from the relation  $\mu_e(t) = (3\pi^2 n_e(t))^{1/3}$ , the kaon chemical potential  $\mu_K(t)$  and the chiral angle  $\theta(t)$  from Eqs.(15)–(18) and (19), and then the difference between  $\mu_p(t)$  and  $\mu_n(t)$  from Eq.(12). Because the charge neutrality condition,  $n_p(t) = n_K(t) + n_e(t)$ , is built into the rate equations (22), it can be seen that this condition is always satisfied. The system evolves dynamically toward an equilibrated kaon-condensed phase through the nonequilibrium weak processes, KU, MU, and KT.

#### IV. NUMERICAL RESULTS AND DISCUSSION

We choose the value for the  $KN$  sigma term to be  $\Sigma_{KN} = 300$  MeV [42]. The critical density  $n_B^C$  is then estimated to be  $n_B^C = 0.49 \text{ fm}^{-3}$  ( $= 3.0 n_0$ ) [c.f. Ref. [43]]. In Table I, we list the values for  $\mu_K^0$  and the proton fraction  $x_p^0$  for the initial noncondensed state ( $t=0$ ), and those of  $\theta$ ,  $\mu_K$  and  $x_p$  for the kaon-condensed state in chemical equilibrium ( $t \rightarrow \infty$ ) [which we denote by the superscript ‘eq’]. It has been shown in Ref. [43] that the temperature dependence of the critical density and physical quantities in the kaon-condensed phase is weak for the temperature less than several tens of MeV. Thus all the values listed in Table I have been estimated at  $T=0$ . Here, we study the temporal behavior of the physical quantities for two different baryon number densities,  $n_B = 0.55 \text{ fm}^{-3}$  and  $0.70 \text{ fm}^{-3}$ . The density  $n_B = 0.55 \text{ fm}^{-3}$  is close to  $n_B^C$ , such that we have a rather weak condensed state with small  $\theta^{\text{eq}}$ . For  $n_B = 0.70 \text{ fm}^{-3}$ , on the other hand, we have a well-developed condensed state with a large order parameter  $\theta^{\text{eq}}$ . When the baryon number density is increased above the critical density for kaon condensation, the number density of negatively-charged kaons increases as the condensate develops. Charge neutrality of the system is maintained by the increase in the proton number density. Consequently, the proton fraction  $x_p^{\text{eq}}$  increases as the baryon number density increases in an equilibrated kaon-condensed state. On the other hand, the negatively charged electrons are replaced by the negatively charged kaons as a condensate develops with an increase in the baryon number density. The consequent decrease in the electron abundance produces a decrease in the charge chemical potential  $\mu_e^{\text{eq}}$  ( $= \mu_K^{\text{eq}}$ ), resulting in a large proton fraction and a reduced charge chemical potential, which are two characteristic features of the kaon-condensed state [2–5].

##### A. Two typical time scales

In Fig.1 (a), we show the chiral angle  $\theta$  as a function of time for  $n_B = 0.55 \text{ fm}^{-3}$  and  $T = 1.0 \times 10^{11} \text{ K}$ . For the initial values,  $\mu_K^0 = -b^0 = -139 \text{ MeV}$  and  $x_p^0 = 0.14$ . The evolution of the kaon condensate may be divided into the following three stages: (I) no condensate ( $\theta(t) = 0$ ) with thermal kaons present until the onset of condensation, (II) onset of condensation and its monotonic growth, and (III) the asymptotic stage

near chemical equilibrium. In equilibrium, one finds  $\theta^{\text{eq}}=0.48$  (rad) from Fig. 1(a), and the kaon chemical potential and the proton fraction have the values  $\mu_K^{\text{eq}}=203$  MeV and  $x_p^{\text{eq}} \equiv n_p^{\text{eq}}/n_B = 0.23$ , respectively (see Table I).

The onset of condensation from a noncondensed state and its subsequent growth are related to the change in shape of the thermodynamic potential  $\Omega$  as a function of  $\theta$  around  $\theta = 0$ . This change in shape is also associated with the appearance of a soft kaon mode, reflected in a singularity of the distribution function  $f_K(\mathbf{p}_K)$ , Eq.(18). To see this, we expand  $\Omega(t)/V$  around  $\theta = 0$ :

$$\Omega(t)/V = -\frac{f^2}{2}\widetilde{D}_K^{-1}\theta(t)^2 + O(\theta(t)^4), \quad (29)$$

with  $\widetilde{D}_K^{-1} \equiv D_K^{-1}(\omega = \mu_K(t), \mathbf{p}_K = 0; n_B)$ , where  $D_K^{-1}(\omega, \mathbf{p}_K; n_B)$  is the inverse kaon propagator:

$$D_K^{-1}(\omega, \mathbf{p}_K; n_B) \equiv \omega^2 - \mathbf{p}_K^2 + 2b(t)\omega - m_K^{*2}. \quad (30)$$

Beginning with  $\mu_K = -b^0$  at  $t=0$ , the kaon chemical potential  $\mu_K(t)$  increases monotonically with time. As a result, the factor  $\widetilde{D}_K^{-1}$  changes sign, depending on the value of  $\mu_K$  relative to the critical value,  $\mu_K^C(t) \equiv -b(t) + (b(t)^2 + m_K^{*2})^{1/2}$ , defined as a root of  $\widetilde{D}_K^{-1}$ . In Fig. 2, we show the thermodynamic potential per particle  $\Omega/(Vn_B)$  as a function of  $\theta$  for  $n_B=0.55$  fm $^{-3}$  and  $T=1.0 \times 10^{11}$  K and the other parameters  $n_i$  and  $\mu_i$  ( $i = p, n, e^-, K^-$ ) fixed at three times corresponding to cases (i)–(iii). Case (i) corresponds to a time before the onset of condensation, for which  $\mu_K$  is smaller than  $\mu_K^C$ . [E.g., at  $t=0$ ,  $\mu_K = -b^0 < \mu_K^C(t=0)$ .] In this case,  $\widetilde{D}_K^{-1}$  is negative, which means that the thermodynamic potential per unit volume  $\Omega/V$  is convex at  $\theta=0$ , as seen from Eq. (29) and the curve (i) in Fig. 2, and the noncondensed state ( $\theta=0$ ) is stable against fluctuations in  $\theta$ . Because  $\mu_K^C$  corresponds to the lowest excitation energy of the  $K^-$ ,  $\omega_-(\mathbf{p}_K = 0)$  *in normal matter*, one can see that  $\omega_-(\mathbf{p}_K) > \omega_-(\mathbf{p}_K = 0) = \mu_K^C > \mu_K$ . Thus the Bose-Einstein distribution function  $f_K$  here has no singularity. Case (ii) corresponds to a time for which  $\mu_K(t) = \mu_K^C(t)$ , where  $\widetilde{D}_K^{-1} = 0$ . In this case, the system becomes unstable with respect to the fluctuations in  $\theta$  (the curve (ii) in Fig. 2), and since  $\omega_-(\mathbf{p}_K = 0) (= \mu_K^C)$  is equal to  $\mu_K$ ,  $f_K(\mathbf{p}_K)$  becomes divergent at  $\mathbf{p}_K=0$ . Thus the appearance of a soft kaon mode with  $\omega_-(\mathbf{p}_K = 0)=\mu_K$  implies the onset of an instability due to the formation of a condensate. Finally, case (iii) corresponds to a time after the onset of condensation, for which  $\mu_K(t)$  exceeds  $\mu_K^C(t)$ , so that  $\widetilde{D}_K^{-1} > 0$ . In this case,  $\Omega/V$  is concave near  $\theta=0$  as a function of  $\theta$ ; which means that the noncondensed state corresponds to the maximum of  $\Omega/V$ , as seen from the curve (iii) in Fig. 2, and is unstable against the formation of a condensate. The system therefore evolves into a condensate described by  $\theta(t)$ , which is determined adiabatically by a minimum in the thermodynamic potential [cf. Eq.(19)]. By the use of the dispersion relations for the kaon *in the condensed phase* (see II B) [38], it can be shown that the lowest excitation energy of  $K^-$  *in the condensed phase* is equal to  $\mu_K$ , i.e.,  $\omega_-(\mathbf{p}_K = 0) = \mu_K(t)$ ; there is a soft kaon mode in the condensed phase, and  $f_K(\mathbf{p}_K)$  is divergent at  $\mathbf{p}_K = 0$ , as in the case (ii). From Fig. 1(b), where  $\widetilde{D}_K^{-1}$  is shown as a function of time, one sees that the function  $\widetilde{D}_K^{-1}$  changes sign at the onset of condensation. We can call the onset time for condensation *the nucleation time*,  $\tau_{\text{nucl}}$ , and the time for growth of the condensate *the coherence time*,  $\tau_{\text{coh}}$ , after Stoof's discussion

about the formation of BEC in an atomic gas [44]. From Fig. 1, one finds  $\tau_{\text{nucl}} = 8 \times 10^{-8}$  sec, and  $\tau_{\text{coh}} = 5 \times 10^{-5}$  sec for  $n_{\text{B}}=0.55 \text{ fm}^{-3}$  and  $T = 1.0 \times 10^{11}$  K.

## B. Connection between the reaction rates and the change in chemical composition

The temporal behavior of the reaction rate for each weak process is shown for  $n_{\text{B}}=0.55 \text{ fm}^{-3}$  and  $T = 1.0 \times 10^{11}$  K in Fig. 3. The solid, dashed and dotted lines denote the KT, MU, and KU processes, respectively. The curves show that the forward thermal kaon process KT-F is dominant in magnitude over the KU and MU reactions throughout the equilibration process [37]. Hence the production of the thermal and condensed kaons proceeds mainly via the KT-F reaction, which is responsible for the onset of condensation and its subsequent growth.

In Fig. 4, we show the temporal behavior of the dimensionless parameters  $\xi^{(\alpha)}$  ( $\alpha = \text{KU, MU, KT}$ ), which measure the deviation from chemical equilibrium. Beginning with a large negative value,  $\xi^{(\text{KT})}$  increases monotonically toward zero, where the system is in chemical equilibrium with respect to the KT reactions. Note that the KT reaction rates are large even in the initial stage where the system is far from chemical equilibrium ( $|\xi^{(\text{KT})}(t)| \gg 1$ ). In Paper I, we examined in detail the characteristic roles of the soft and hard thermal kaons in the KT reactions, and demonstrated that the high-energy component of the thermal kaons contributes to the KT reaction rates during the noncondensed stage. On the other hand, a low energy component (a soft mode) of the thermal kaon excitations in the kaon-condensed state was shown to contribute mainly near chemical equilibrium [37].

Let us now examine how these reactions change the chemical composition. The number densities of the chemical species are shown in Fig. 5 for the same density and temperature as in Figs. 1–4. In stage I ( $0 < t < \tau_{\text{nucl}}$ ), where there is no condensate, the kaons produced by the KT reactions are thermal, and the KU reactions cannot proceed because there is no condensate ( $\theta = 0$ ). The initial  $\beta$ -equilibrium is disturbed by the proton excess, created through the KT-F reaction, and the MU reactions are enhanced because the MU-B reaction proceeds more rapidly than the MU-F reaction, which restores  $\beta$ -equilibrium by reducing the proton excess. Nevertheless, the proton number density  $n_p$  still increases, since the KT-F reaction rate is larger than the MU-B reaction rate, as can be seen in Fig. 3 (see also Paper I). Because the total baryon number density  $n_{\text{B}}$  is constant, the neutron number density  $n_n$  therefore decreases with time. In stage I, the change in the electron number density  $n_e$  is brought about only by the MU reactions, and  $n_e$  decreases slightly with time, the MU-B reaction proceeding more rapidly than the MU-F reaction. The extent of the changes in  $n_p$ ,  $n_n$ , and  $n_e$  is very small. Consequently, although the electron chemical potential  $\mu_e$  decreases with time because of the decrease in  $n_e$ , this potential, along with the proton and the neutron chemical potentials  $\mu_p$  and  $\mu_n$  remain almost constant in stage I. On the other hand, the kaon chemical potential  $\mu_K$  increases significantly with time;  $\mu_K^0 = -b^0$  at  $t=0$  and  $\mu_K \simeq \mu_K^{\text{eq}}$  at  $t = \tau_{\text{nucl}}$ . Hence  $\xi^{(\text{KU})}$ , which is proportional to  $\mu_e - \mu_K$ , decreases monotonically with time and  $\xi^{(\text{KT})}$  increases monotonically with time [cf. Fig. 4], while  $\xi^{(\text{MU})}$  remains close to its initial value ( $\sim 0$ ) except for the time near  $\tau_{\text{nucl}}$ .

In stage II ( $\tau_{\text{nucl}} < t < \tau_{\text{coh}}$ ), the KU reactions can proceed due to the appearance of a condensate, but the qualitative behavior of each chemical composition is similar to stage

I. In particular, the kaon and proton number densities increase through the KT reactions, while those of the electrons and neutrons decrease. The change in the number density of the kaons  $n_K$  comes mainly from the condensed part  $\zeta_K$  [(15)] after the saturation of the thermal part  $n_K^T$ , with the condensed part  $\zeta_K$  roughly proportional to the square of  $\theta$ ,  $\zeta_K \propto \theta^2$ , for a small chiral angle, as seen from Eq. (16). According to Fig.1(a), the chiral angle  $\theta$  increases rapidly with time for  $t \gtrsim \tau_{\text{nucl}}$ . Thus the change in the number density of the kaons  $n_K$  is substantial, being more pronounced in stage II than in stage I due to the appearance of a condensate. The change in the number density of the electrons  $n_e$  in stage II is caused by the KU and MU reactions. But since the reaction rates for the electron absorption processes, KU-B and MU-B, are smaller by orders of magnitude than the rate for the kaon production process KT-F, the change in the number density of the electrons is less marked than the change in the number density of the kaons, and remains almost constant near the onset of condensation, until both the MU-B and KU-B reactions become maximum and operate significantly to reduce  $n_e$  in the later part of stage II (cf. Figs. 3 and 5). From the temporal behaviors of  $n_K$ ,  $n_e$ , the charge neutrality,  $n_p = n_e + n_K$ , and baryon number conservation,  $n_p + n_n = n_B$ , it can be seen that the change in the number densities of the protons and neutrons become remarkable in stage II.

During the earlier part of stage II where the number density of the electrons is almost constant, the parameter  $\xi^{(\text{KU})}$  remains unchanged because both the electron and the kaon chemical potentials are almost constant. On the other hand, as a result of the increase in the proton number density and the decrease in the neutron number density, the difference between the proton and neutron chemical potentials becomes larger with time, as seen from Eq.(12). Thus the parameter  $\xi^{(\text{MU})}$  increases with time, after which both  $\xi^{(\text{KU})}$  and  $\xi^{(\text{MU})}$  decrease with time, and the system enters into the final stage III (cf. Fig. 4).

The coherence time  $\tau_{\text{coh}}$  may be identified with the time at which the magnitudes of the forward and backward reaction rates for KT become equal. As seen in Fig.3, chemical equilibrium with respect to the KU and MU reactions is achieved at a later time than that at which the KT reaction reaches equilibrium.

Finally, in stage III ( $t > \tau_{\text{coh}}$ ), where the system is close to chemical equilibrium ( $\xi^{(\text{KT})} \simeq 0$ ), both the KU and MU reactions compete with each other to determine the dynamical behavior of the system. In this stage, the deviation parameters  $\xi^{(\text{KU})}$  and  $\xi^{(\text{MU})}$  damp exponentially with time, and the system approaches chemical equilibrium. The relaxation time  $\tau_{\text{rel}}$  can be calculated analytically [see Eq. (A11) in Appendix A]. For  $n_B=0.55 \text{ fm}^{-3}$  and  $T=1.0 \times 10^{11} \text{ K}$ , the analytic result gives  $\tau_{\text{rel}} = 2 \times 10^{-4} \text{ sec}$ , which is in agreement with the numerical result read from Fig. 3.

### C. Temperature-dependence of the characteristic time scales

Next we compare the temperature dependence of the characteristic time scales,  $\tau_{\text{nucl}}$ ,  $\tau_{\text{coh}}$ , and  $\tau_{\text{rel}}$  at a fixed baryon number density. Figure 6 shows the behavior of the chiral angle  $\theta$  for  $n_B=0.55 \text{ fm}^{-3}$  at three different temperatures,  $T = 1.0 \times 10^{10} \text{ K}$ ,  $1.0 \times 10^{11} \text{ K}$ , and  $5.0 \times 10^{11} \text{ K}$ . In addition, Table II lists the values of  $\tau_{\text{nucl}}$  and  $\tau_{\text{coh}}$ , estimated from the numerical calculations, and the value of  $\tau_{\text{rel}}$ , obtained from Eq. (A11). Roughly speaking, it can be seen that  $\tau_{\text{nucl}}$  depends weakly on temperature, while  $\tau_{\text{coh}}$  and  $\tau_{\text{rel}}$

depend sensitively on temperature: In particular, from Table II and Fig. 6, one obtains  $\tau_{\text{nucl}}=2 \times 10^{-8}$  sec  $\rightarrow 6 \times 10^{-9}$  sec,  $\tau_{\text{coh}}=2 \times 10^{-1}$  sec  $\rightarrow 4 \times 10^{-8}$  sec, and  $\tau_{\text{rel}}=40$  sec  $\rightarrow 5 \times 10^{-7}$  sec as  $T = 1.0 \times 10^{10}$  K  $\rightarrow 5.0 \times 10^{11}$  K for  $n_B=0.55$  fm $^{-3}$ .

Consider first the temperature dependence of the nucleation time,  $\tau_{\text{nucl}}$ , which provides a typical time scale for saturation of the thermal part of the strangeness number density  $n_K^T(t)$ . For  $t > \tau_{\text{nucl}}$ ,  $n_K^T(t)$  changes little. In chemical equilibrium, the thermal kaons occupy a progressively larger part of the total strangeness density as the temperature increases, and two competing effects produce the temperature dependence of  $\tau_{\text{nucl}}$ . (i) The value of  $n_K^T(t)$  at saturation is larger at higher temperature, which tends to increase the nucleation time,  $\tau_{\text{nucl}}$ . On the other hand, (ii) a higher temperature gives a higher reaction rate for the relevant KT process. (cf. Paper I). As a consequence the thermal kaon number density  $n_K^T(t)$  comes to saturation earlier.

In contrast, the temperature dependence of the coherence time  $\tau_{\text{coh}}$  is explained by the fact that after a condensate appears, its subsequent growth in stage II is controlled mainly by the KT reactions, as seen in Sec. IV B, and the KT reaction rates depend sensitively on the temperature over the entire nonequilibrium processes, (cf. Paper I). This leads to a sensitive temperature dependence of  $\tau_{\text{coh}}$ .

Finally, the relaxation time  $\tau_{\text{rel}}$  depends on the KU and MU reaction rates through the quantities  $\tilde{\Gamma}^{(\text{KU-F})}$  ( $\propto T^5$ ) and  $\tilde{\Gamma}^{(\text{MU-F})}$  ( $\propto T^7$ ) [see Eq. (A9) in Appendix A], and from Eqs. (A11) and (A9), it can be seen that the relaxation time  $\tau_{\text{rel}}$  depends sensitively on the temperature, so as to decrease significantly as the temperature increases.

#### D. Density-dependence of the characteristic time scales

Here we discuss the temporal behavior of the system at a higher baryon number density,  $n_B=0.70$  fm $^{-3}$ , for which one can expect a fully developed kaon-condensed phase when the system is in chemical equilibrium. Initially we start with  $n_K^T(t=0) = 0$ , which gives  $\mu_K^0 = -b^0 = -180$  MeV and  $x_p^0=0.16$ . The temporal behavior of the chiral angle  $\theta$  is shown in Fig. 7 for  $n_B=0.70$  fm $^{-3}$  for the same three temperatures as in Fig. 6. The numerical values for the nucleation time  $\tau_{\text{nucl}}$ , the coherence time  $\tau_{\text{coh}}$ , and the relaxation time  $\tau_{\text{rel}}$  for the density and temperatures corresponding to the three curves shown are listed in Table II. From an examination of this table and Fig. 7, it can be seen that while the nucleation time  $\tau_{\text{nucl}}$  depends weakly on the temperature, the coherence time  $\tau_{\text{coh}}$  and the relaxation time  $\tau_{\text{rel}}$  depend sensitively on the temperature, becoming shorter as the temperature is raised. These features for  $\tau_{\text{nucl}}$ ,  $\tau_{\text{coh}}$ , and  $\tau_{\text{rel}}$  are qualitatively the same as in the case of the lower baryon number density  $n_B=0.55$  fm $^{-3}$ .

The time scales obtained for  $n_B=0.70$  fm $^{-3}$  can be compared with those for  $n_B=0.55$  fm $^{-3}$ . From Table II, one can see that the nucleation time  $\tau_{\text{nucl}}$  is sensitive to the baryon number density, with the ratio  $\tau_{\text{nucl}}(0.55 \text{ fm}^{-3})/\tau_{\text{nucl}}(0.70 \text{ fm}^{-3})$  equal to  $2 \times 10 - 2 \times 10^3$  for  $1 \times 10^{10}$  K  $< T < 5 \times 10^{11}$  K. This density dependence is explained as follows: In the noncondensed state where  $|\xi^{(\text{KT})}| \gg 1$  ( $\xi^{(\text{KT})} < 0$ ), the KT-F reaction rate is very sensitive to  $|\xi^{(\text{KT})}|$  and becomes large rapidly as  $|\xi^{(\text{KT})}|$  increases [37]. In addition, the kaon chemical potential  $\mu_K$  ( $< 0$  at  $t = 0$ ) in  $|\xi^{(\text{KT})}|$  increases rapidly with time in stage I, and, before the onset of condensation, it is already almost equal to the equilibrium value  $\mu_K^{\text{eq}}$  ( $> 0$ ), which has a smaller value for a larger baryon number density. As compared

with the density dependence of  $\mu_K$ , the density dependence of the difference between the proton and neutron chemical potentials  $\mu_p - \mu_n$  ( $< 0$ ) in  $|\xi^{(\text{KT})}|$  is weak. Hence, as the baryon number density increases, the parameter  $|\xi^{(\text{KT})}|$  ( $=|\mu_K + \mu_p - \mu_n|/T \gg 1$ ) increases mainly due to the decrease in  $\mu_K$ . As a result, the KT-F reaction rate in stage I is much larger for a larger baryon number density, which considerably reduces the time required for saturation of the thermal kaon number density.

After the appearance of a condensate, the value of  $|\xi^{(\text{KT})}|$  becomes sufficiently small, so that the density dependence of  $|\xi^{(\text{KT})}|$  becomes insignificant. Therefore, the KT-F reaction rate does not depend much on  $n_B$ . Hence the coherence time  $\tau_{\text{coh}}$ , which is controlled by the KT-F reaction, shows only a weak dependence on  $n_B$ . In a similar way, near chemical equilibrium where  $|\xi^{(\text{KU})}| \ll 1$  and  $|\xi^{(\text{MU})}| \ll 1$ , the density dependence of both the KU-F and MU-F reaction rates is weak, and therefore  $\tau_{\text{rel}}$ , which is determined by these reaction rates, is found to have a weak dependence on  $n_B$ .

### E. Implications for the delayed collapse of a neutron star

From Table II, one can see that a condensate develops fully with a characteristic time scale given by the coherence time  $\tau_{\text{coh}}$ . In the context of the delayed collapse of a newly born neutron star, we consider some implications of the results. Since the neutrino degeneracy is not taken into account in our framework, our results are applicable to the cooling era after the deleptonization. Hence the delayed collapse associated with a kaon condensate should be considered in this cooling era.

The low temperature case (e.g.,  $T = 1 \times 10^{10}$  K) may apply to the final stage of the cooling era, while the high temperature case (e.g.,  $T \gtrsim 10^{11}$  K) to the initial stage. In both cases, we have found that the time scale of  $\tau_{\text{coh}}$  is very small;  $\tau_{\text{coh}} \sim 0.1$  sec for  $T = 1 \times 10^{10}$  K and  $\tau_{\text{coh}} \lesssim 5 \times 10^{-5}$  sec for  $T \gtrsim 10^{11}$  K, which should be compared with the cooling time scale of order of ten seconds. Hence we can conclude that, in both cases, the time delay of a collapse due to the formation of a condensate is negligible as compared with the cooling time scale and will have a minor effect on the evolution of the protoneutron star.

## V. SUMMARY AND CONCLUDING REMARKS

We have considered the kinetics of kaon condensation by the use of rate equations which include the three weak reactions: the thermal kaon process, the kaon-induced Urca process, and the modified Urca process. The thermal kaon process is shown to be dominant over other weak reactions throughout the equilibration process. The evolution of the kaon condensate is divided into the following three stages: (I) the noncondensed stage before the onset of condensation, (II) onset of condensation and its growth until its saturation, and (III) the asymptotic relaxation stage near chemical equilibrium. The role of thermal kaons and especially the connection between the existence of a soft kaon mode and the instability of the noncondensed state has been clarified. It has been found that a full development of a condensate is characterized by a time scale given by the coherence time  $\tau_{\text{coh}}$ . Using these results, we have made a brief comment on implications of our results on the delayed collapse mechanism of a newly-born neutron star into a black hole.



The situation adopted in our framework may be applicable to the cooling era after the deleptonization. It is found that the time scale of the development of a condensate (the coherence time) is much smaller than that of the cooling for the relevant temperatures (1 MeV– several tens of MeV). Therefore, the time delay for the formation of a kaon condensate may not affect the delayed collapse of a neutron star.

Several effects which should be taken into account within our framework in the future are as follows:

(1) We have used the thermodynamic potential neglecting any fluctuations except for those produced by thermal kaons. However, for a neutron star just born in a supernova, since the initial temperature is as high as several tens of MeV, thermal fluctuations other than the kaon thermal loop contributions [38] should be fully incorporated into the thermodynamic potential.

(2) Furthermore, since the matter is opaque to the neutrinos at high temperatures, the thermal effects associated with neutrino diffusion may also be important. In particular, the degenerate neutrinos will contribute to the thermodynamic potential and influence the relevant reaction rates. Therefore, the neutrino diffusion may affect the thermal evolution of a newly-born neutron star.

(3) The reaction rates for the relevant weak processes have been obtained in the low temperature approximation (c.f. Paper I). The expressions for the reaction rates must be extended to the high temperature case, and the phase-space integrals should be performed numerically beyond the low temperature approximation [46].

(4) During the equilibration process, we have assumed that the temperature  $T$  is constant: the energy produced by the weak reactions is lost to the surroundings. However, because the energy release due to the nonequilibrium weak reactions will heat up the matter, the temperature is in general time-dependent during the course of the equilibration process, and this can affect the evolution of the star. This thermal effect can be included through an additional equation that determines the rate of change of the internal energy of the system.

<sup>5</sup> A significant increase in the temperature could possibly lead to further reduction of the time scale for the growth of a condensate represented by the coherence time. On the other hand, as a result of the raise in the temperature, the critical density  $n_B^C$  for kaon condensation can be pushed up to higher density, which may cause the delay in the onset of condensation. In this respect, it is necessary to obtain a phase diagram in the  $T - n_B$  plane [38,43], and the dynamics of the onset and growth of condensation must be considered along a trajectory in this plane.

## VI. ACKNOWLEDGEMENTS

The authors wish to thank M. Yasuhira for discussions. We are grateful to Professor R.T.Deck for comments on the manuscript. One of the authors (T.M.) thanks for support

---

<sup>5</sup> In Ref. [46], strangeness production in quark matter has been considered with allowance for the time dependence of the temperature. It has been shown that the temperature changes appreciably with time up to  $\sim 50$  MeV during the nonequilibrium process, and that the time scale for saturation of the strangeness in this case is smaller by orders of magnitude than the case where the temperature is held fixed.

through the Grant-in-Aid of Chiba Institute of Technology (C.I.T). Numerical calculations were carried out on the DEC Alpha Server 4100 System, C.I.T. This material is based upon work supported in part by the National Science Foundation through the Theoretical Physics Program under Grant Nos.PHY9008475 and PHY9722138, and by the Japanese Grant-in-Aid for Scientific Research Fund of the Ministry of Education, Science, Sports and Culture (08640369,11640272).

## APPENDIX A: ASYMPTOTIC BEHAVIOR NEAR CHEMICAL EQUILIBRIUM

We derive an expression for the relaxation time which characterizes the asymptotic behavior of the system near chemical equilibrium (stage III).

### 1. Linearization of $\xi^{(\text{KU})}(t)$ and $\xi^{(\text{MU})}(t)$

In stage III, both the forward and backward KT reaction rates are almost equal, i.e.,  $\xi^{(\text{KT})}(t) \simeq 0$ . Therefore, we consider the case where the relaxation proceeds only through the KU and MU reactions, neglecting the KT reaction. The parameters  $\xi^{(\text{KU})}(t)$  and  $\xi^{(\text{MU})}(t)$  are written as

$$\xi^{(\text{KU})}(t) = [\delta\mu_e(t) - \delta\mu_K(t)]/T, \quad (\text{A1a})$$

$$\xi^{(\text{MU})}(t) = [\delta\mu_e(t) + \delta\mu_p(t) - \delta\mu_n(t)]/T, \quad (\text{A1b})$$

where  $\delta\mu_i(t)$  ( $i = p, n, e^-, K^-$ ) is the deviation of the chemical potential from the equilibrium value, i.e.,  $\delta\mu_i(t) = \mu_i(t) - \mu_i^{\text{eq}}$ . From the relation,  $\mu_e = (3\pi^2 n_e)^{1/3}$ , one obtains

$$\delta\mu_e(t) = (\pi/\mu_e^{\text{eq}})^2 \delta n_e(t), \quad (\text{A2})$$

where  $\delta n_e(t) = n_e(t) - n_e^{\text{eq}}$ . One can also write the deviations of the chemical potentials  $\delta\mu_K(t)$  and  $\delta\mu_p(t) - \delta\mu_n(t)$  in terms of  $\delta n_i(t)$  ( $=n_i(t) - n_i^{\text{eq}}$ ) from linearized forms of the three equations with respect to  $\delta\mu_K(t)$ ,  $\delta\theta(t)$ ,  $\delta\mu_p(t) - \delta\mu_n(t)$ , and  $\delta n_i(t)$  represented by: the expression for the kaon number density [Eq. (15)], the classical field equation [Eq. (19)], and the expression for the difference between  $\mu_p$  and  $\mu_n$  [Eq. (12)]. Note that we can neglect the deviation of the thermal kaon part in the kaon number density, i.e.,  $\delta n_K(t) = \delta\zeta_K(t)$  ( $\delta n_K^T(t) = 0$ ), because the thermal kaon number density  $n_K^T(t)$  is almost constant after a condensate appears until the system reaches chemical equilibrium.

The deviation of the electron number density  $\delta n_e(t)$  is divided into two contributions:

$$\delta n_e(t) = \delta^{(\text{KU})} n_e(t) + \delta^{(\text{MU})} n_e(t), \quad (\text{A3})$$

where  $\delta^{(\text{KU})} n_e(t)$  [ $\delta^{(\text{MU})} n_e(t)$ ] is caused by the KU reactions (the MU reactions). The number densities for the other species are related to  $\delta^{(\text{KU})} n_e(t)$  and  $\delta^{(\text{MU})} n_e(t)$  by

$$\delta n_K(t) = -\delta^{(\text{KU})} n_e(t), \quad (\text{A4a})$$

$$\delta n_p(t) = \delta^{(\text{MU})} n_e(t), \quad (\text{A4b})$$

$$\delta n_n(t) = -\delta n_p(t) = -\delta^{(\text{MU})} n_e(t) \quad (\text{A4c})$$

Following the above results, the deviation parameters (A1) can be expressed in terms of  $\delta^{(\text{KU})}n_e(t)$  and  $\delta^{(\text{MU})}n_e(t)$ . The result is

$$\xi^{(\text{KU})}(t) = \frac{p}{T}\delta^{(\text{KU})}n_e(t) + \frac{q}{T}\delta^{(\text{MU})}n_e(t) , \quad (\text{A5a})$$

$$\xi^{(\text{MU})}(t) = \frac{q}{T}\delta^{(\text{KU})}n_e(t) + \frac{r}{T}\delta^{(\text{MU})}n_e(t) , \quad (\text{A5b})$$

where

$$p = \left[ \left( \frac{\pi}{\mu_e} \right)^2 + \frac{1}{f^2 \{ \sin^2 \theta + 4(\cos \theta + b/\mu_K)^2 \}} \right]^{\text{eq}} , \quad (\text{A6a})$$

$$q = \left[ \left( \frac{\pi}{\mu_e} \right)^2 + \frac{1 + \cos \theta + 2b/\mu_K}{2f^2 \{ \sin^2 \theta + 4(\cos \theta + b/\mu_K)^2 \}} \right]^{\text{eq}} , \quad (\text{A6b})$$

$$r = \left[ \left( \frac{\pi}{\mu_e} \right)^2 + \frac{(1 - \cos \theta)(\cos \theta + 2b/\mu_K)}{2f^2 \{ \sin^2 \theta + 4(\cos \theta + b/\mu_K)^2 \}} + \frac{2(3\pi^2)^{2/3}}{3 \cdot 2m_N} (n_p^{-1/3} + n_n^{-1/3}) + \frac{8V_{\text{sym}}(n_B)}{n_B} \right]^{\text{eq}} . \quad (\text{A6c})$$

In Eq.(A6), the first term comes from the deviation of the electron chemical potential  $\delta\mu_e$ , (A2), and the second term from the deviation of the parameters for a condensate, i.e.,  $\delta\mu_K$  and  $\delta\theta$ . The third and fourth terms in Eq. (A6c) come from the deviation of the proton and neutron chemical potentials. It is to be noted that a condensate already develops fully in stage III, so that the quantities for the condensate are almost constant. Thus it is a good approximation to set  $\delta\mu_K = \delta\theta = 0$ , which leads to  $p = q \simeq \left( \frac{\pi}{\mu_e^{\text{eq}}} \right)^2$ ,

$$\text{and } r \simeq \left[ \left( \frac{\pi}{\mu_e} \right)^2 + \frac{2(3\pi^2)^{2/3}}{3 \cdot 2m_N} (n_p^{-1/3} + n_n^{-1/3}) + \frac{8V_{\text{sym}}(n_B)}{n_B} \right]^{\text{eq}} .$$

## 2. Differential equations for $\xi^{(\text{KU})}(t)$ and $\xi^{(\text{MU})}(t)$

By differentiating both sides of Eq. (A5) with time, one finds that the rates of change of  $\xi^{(\text{KU})}(t)$  and  $\xi^{(\text{MU})}(t)$  are related to the reaction rates for KU and MU, through the rate equations

$$\frac{d}{dt}\delta^{(\text{KU})}n_e(t) = \Gamma^{(\text{KU-F})}(\xi^{(\text{KU})}(t), T) - \Gamma^{(\text{KU-F})}(-\xi^{(\text{KU})}(t), T) , \quad (\text{A7a})$$

$$\frac{d}{dt}\delta^{(\text{MU})}n_e(t) = \Gamma^{(\text{MU-F})}(\xi^{(\text{MU})}(t), T) - \Gamma^{(\text{MU-F})}(-\xi^{(\text{MU})}(t), T) . \quad (\text{A7b})$$

For the system close to chemical equilibrium,  $|\xi^{(\text{KU})}(t)| \ll 1$  and  $|\xi^{(\text{MU})}(t)| \ll 1$ . In this case, the r.h.s. of Eqs. (A7a) and (A7b) can be expanded up to first order in  $\xi^{(\text{KU})}(t)$  and  $\xi^{(\text{MU})}(t)$ , respectively. Thus one obtains the coupled differential equations for  $\xi^{(\text{KU})}(t)$  and  $\xi^{(\text{MU})}(t)$ :

$$\frac{d}{dt}\xi^{(\text{KU})}(t) = -\frac{p}{T}\tilde{\Gamma}^{(\text{KU-F})} \cdot \xi^{(\text{KU})}(t) - \frac{q}{T}\tilde{\Gamma}^{(\text{MU-F})} \cdot \xi^{(\text{MU})}(t) , \quad (\text{A8a})$$

$$\frac{d}{dt}\xi^{(\text{MU})}(t) = -\frac{q}{T}\tilde{\Gamma}^{(\text{KU-F})} \cdot \xi^{(\text{KU})}(t) - \frac{r}{T}\tilde{\Gamma}^{(\text{MU-F})} \cdot \xi^{(\text{MU})}(t) , \quad (\text{A8b})$$

where

$$\tilde{\Gamma}^{(\text{KU-F})} \equiv 2 \frac{|I_2'(0)|}{I_2(0)} \Gamma^{(\text{KU-F})}(\xi^{(\text{KU})} = 0, T) \simeq 1.3 \times \Gamma^{(\text{KU-F})}(\xi^{(\text{KU})} = 0, T) \propto T^5, \quad (\text{A9a})$$

$$\tilde{\Gamma}^{(\text{MU-F})} \equiv 2 \frac{|J_2'(0)|}{J_2(0)} \Gamma^{(\text{MU-F})}(\xi^{(\text{MU})} = 0, T) \simeq 1.2 \times \Gamma^{(\text{MU-F})}(\xi^{(\text{MU})} = 0, T) \propto T^7, \quad (\text{A9b})$$

with  $I_2(0) = \frac{3}{2}\pi^2\zeta(3) + \frac{45}{2}\zeta(5) = 41.13$ ,  $I_2'(0) \equiv (dI_2(u)/du)_{u=0} = -\frac{17}{60}\pi^4$ ,  $J_2(0) = \frac{27}{2}\pi^4\zeta(3) + 225\pi^2\zeta(5) + \frac{2835}{4}\zeta(7) = 4598$ , and  $J_2'(0) \equiv (dJ_2(u)/du)_{u=0} = -\frac{367}{126}\pi^6$ . From Eq. (A8), one obtains the following forms of the solutions:

$$\xi^{(\text{KU})}(t) = C_1 e^{-t/\tau_a} + C_2 e^{-t/\tau_b}, \quad (\text{A10a})$$

$$\xi^{(\text{MU})}(t) = C_3 e^{-t/\tau_a} + C_4 e^{-t/\tau_b}, \quad (\text{A10b})$$

where  $C_1 - C_4$  are constants, and  $\tau_a$  and  $\tau_b$  are time constants which characterize the asymptotic evolution of the system. The relaxation time  $\tau_{\text{rel}}$  is defined as the larger of  $\tau_a$  and  $\tau_b$ , and one obtains

$$\tau_{\text{rel}} = \frac{T p \tilde{\Gamma}^{(\text{KU-F})} + r \tilde{\Gamma}^{(\text{MU-F})} + \left[ \{p \tilde{\Gamma}^{(\text{KU-F})} - r \tilde{\Gamma}^{(\text{MU-F})}\}^2 + 4q^2 \tilde{\Gamma}^{(\text{KU-F})} \tilde{\Gamma}^{(\text{MU-F})} \right]^{1/2}}{2 (pr - q^2) \tilde{\Gamma}^{(\text{KU-F})} \tilde{\Gamma}^{(\text{MU-F})}}. \quad (\text{A11})$$

## REFERENCES

- [1] D. B. Kaplan and A. E. Nelson, Phys. Lett. **B175**, 57 (1986); **B179**, 409(E) (1986).  
A. E. Nelson and D. B. Kaplan, Phys. Lett. **B192**, 193 (1987).
- [2] For a review, T. Tatsumi, Prog. Theor. Phys. Suppl. **120** (1995) 111.
- [3] H. Fujii, T. Maruyama, T. Muto and T. Tatsumi, Nucl. Phys. **A597**,645 (1996).
- [4] C. -H. Lee, Phys. Rep. **275**,197 (1996).
- [5] M. Prakash, I. Bombaci, M. Prakash, P. J. Ellis, J. M. Lattimer, R. Knorren, Phys. Rep. **280**, 1 (1997).
- [6] G. E. Brown, C.- H. Lee and R. Rapp, Nucl. Phys. **A639**, 455c(1998).
- [7] V. Koch, Phys. Lett. **B337**, 7 (1994).
- [8] T. Waas,N. Kaiser and W. Weise, Phys. Lett. **B365**,12 (1996); **B379**, 34 (1996).  
T. Waas and W. Weise, Nucl.Phys. **A625**, 287 (1997).
- [9] M. Lutz, Phys. Lett. **B426**, 12 (1998).
- [10] C. J. Batty, E. Friedman and A. Gal, Phys. Rep. **287**, 385 (1997).
- [11] J. Schaffner-Bielich, I. N. Mishustin and J. Bondorf, Nucl. Phys. **A625**, 325 (1997).
- [12] G. Q. Li, C.- H. Lee and G. E. Brown, Phys. Rev. Lett. **79**, 5214 (1997);  
Nucl. Phys. **A625**, 372 (1997).
- [13] W. Cassing and E. L. Bratkovskaya, Phys. Rep. **308**, 65 (1999).
- [14] For a review, P. Senger and H. Ströbele, J. Phys. **G25**, R59 (1999).
- [15] G. Song, B.- A. Li and C. M. Ko, Nucl. Phys. **A646**, 481 (1999).
- [16] V. Thorsson, M. Prakash and J. M. Lattimer, Nucl. Phys. **A572**, 693 (1994).
- [17] G. E. Brown, K. Kubodera, D. Page and P. Pizzocherro, Phys. Rev. **D37**, 2042 (1988).
- [18] T. Tatsumi, Prog. Theor. Phys. **80**, 22 (1988).
- [19] D. Page and E. Baron, Astrophys. J. **254**, L17 (1990).
- [20] H. Fujii, T. Muto, T. Tatsumi and R. Tamagaki, Nucl. Phys. **A571**,758 (1994);  
Phys. Rev. **C50**, 3140 (1994).
- [21] G. E. Brown and H. A. Bethe, Astrophys. J. **423**, 659 (1994).
- [22] T. W. Baumgarte, S. L. Shapiro and S. Teukolsky, Astrophys. J. **443**, 717 (1995);  
**458**, 680 (1996).
- [23] T. Harada, K. Nakano, T. Tatsumi and M. Yasuhira, in preparation.
- [24] T. Takatsuka, Prog. Theor. Phys. **80**, 361 (1988); *ibid* **82**,475 (1989);  
in *The Structure and Evolution of Neutron Stars, Kyoto,1990*, edited by D. Pines,  
R. Tamagaki, and S. Tsuruta (Addison-Wesley, California,1992), p.257.
- [25] M. Takahara and K. Sato, Prog. Theor. Phys. **80**,861 (1988).
- [26] O. G. Benvenuto and J. E. Horvath, Phys. Rev. Lett. **63**, 716 (1989).
- [27] W. Keil and H.-Th. Janka, Astron. Astrophys. **296**,145 (1995).
- [28] J. A. Pons, et al, Astrophys. J. **513**, 780 (1999).
- [29] A. Akmal, V. R. Pandharipande, and D. G. Ravenhall, Phys. Rev. **C58**, 1804 (1998).
- [30] J. W. Percival et al., Astrophys. J. **446**, 832 (1995).
- [31] T. Muto, T. Tatsumi, and N. Iwamoto, Aust. J. Phys. **50**, 13 (1997).
- [32] B. L. Friman and O. V. Maxwell, Astrophys. J. **232**, 541 (1979).
- [33] O. V. Maxwell, Astrophys. J. **316**, 691 (1987).
- [34] J. Boguta, Phys. Lett. **B106**, 255 (1981).
- [35] J. M. Lattimer, C. J. Pethick, M. Prakash, and P. Haensel, Phys. Rev. Lett. **66**, 2701 (1991).

- [36] M. Prakash, M. Prakash, J. M. Lattimer, and C. J. Pethick, *Astrophys. J.* **390**, L77 (1992).
- [37] T. Muto, T. Tatsumi, and N. Iwamoto, preprint nucl-th/9906024, (Paper I).
- [38] T. Tatsumi, Proc.of the APCTP workshop on “Astro-hadron physics”, ed. by G. E. Brown et al. (World Scientific, 1999), p.594.  
T. Tatsumi and M. Yasuhira, *Phys. Lett.* **B441**, 9 (1998); *Nucl. Phys.* **A653**,133 (1999); nucl-th/9904038.
- [39] M. Prakash, T. L. Ainsworth and J. M. Lattimer, *Phys. Rev. Lett.* **61**, 2518 (1988).
- [40] V. Thorsson and P. J. Ellis, *Phys. Rev.* **D55**, 5177 (1997).
- [41] P. Haensel, *Astron. Astrophys.* **262**,131 (1992).
- [42] J. F. Donoghue and C. R. Nappi, *Phys. Lett.* **B168**, 105 (1986).  
R. L. Jaffe and C. L. Korpa, *Commun. Nucl. Part. Phys.* **17**, 163 (1987).
- [43] M. Yasuhira and T. Tatsumi, proceedings of PANIC 99 (KUNS-1589, nucl-th 9908064).
- [44] H. T. C. Stoof, in *Bose-Einstein Condensation*, edited by A. Griffin, D. W. Snoke, and S. Stringari (Cambridge University Press, Cambridge, U.K.,1995), p.226.
- [45] R. F. Sawyer, *Astrophys. J.* **237**, 187 (1980).
- [46] S. K. Ghosh, S. C. Phatak and P. K. Sahu, *Nucl. Phys.* **A596**, 670 (1996).

TABLES

TABLE I. Quantities for the initial noncondensed state ( $t = 0$ ) and for the chemically equilibrated state ( $t \rightarrow \infty$ ). The former (the latter) quantities are denoted by the superscript ‘0’ (‘eq’). All the values are estimated at  $T=0$ .

$n_B(\text{fm}^{-3})$	$\mu_K^0$ ( MeV )	$x_p^0$	$\theta^{\text{eq}}$ (rad)	$\mu_K^{\text{eq}}$ ( MeV )	$x_p^{\text{eq}}$
0.55	-139	0.14	0.48	203	0.23
0.70	-180	0.16	0.91	114	0.39

TABLE II. The nucleation time  $\tau_{\text{nucl}}$ , the coherence time  $\tau_{\text{coh}}$ , and the relaxation time  $\tau_{\text{rel}}$  for different densities and temperatures.

$n_B(\text{fm}^{-3})$	T (K)	$\tau_{\text{nucl}}$ (sec)	$\tau_{\text{coh}}$ (sec)	$\tau_{\text{rel}}$ (sec)
0.55	$1 \times 10^{10}$	$2 \times 10^{-8}$	$2 \times 10^{-1}$	$4 \times 10$
	$1 \times 10^{11}$	$8 \times 10^{-8}$	$5 \times 10^{-5}$	$2 \times 10^{-4}$
	$5 \times 10^{11}$	$6 \times 10^{-9}$	$4 \times 10^{-8}$	$5 \times 10^{-7}$
0.70	$1 \times 10^{10}$	$1 \times 10^{-11}$	$6 \times 10^{-2}$	$9 \times 10$
	$1 \times 10^{11}$	$3 \times 10^{-10}$	$1 \times 10^{-5}$	$2 \times 10^{-4}$
	$5 \times 10^{11}$	$3 \times 10^{-10}$	$2 \times 10^{-8}$	$1 \times 10^{-7}$

FIGURES

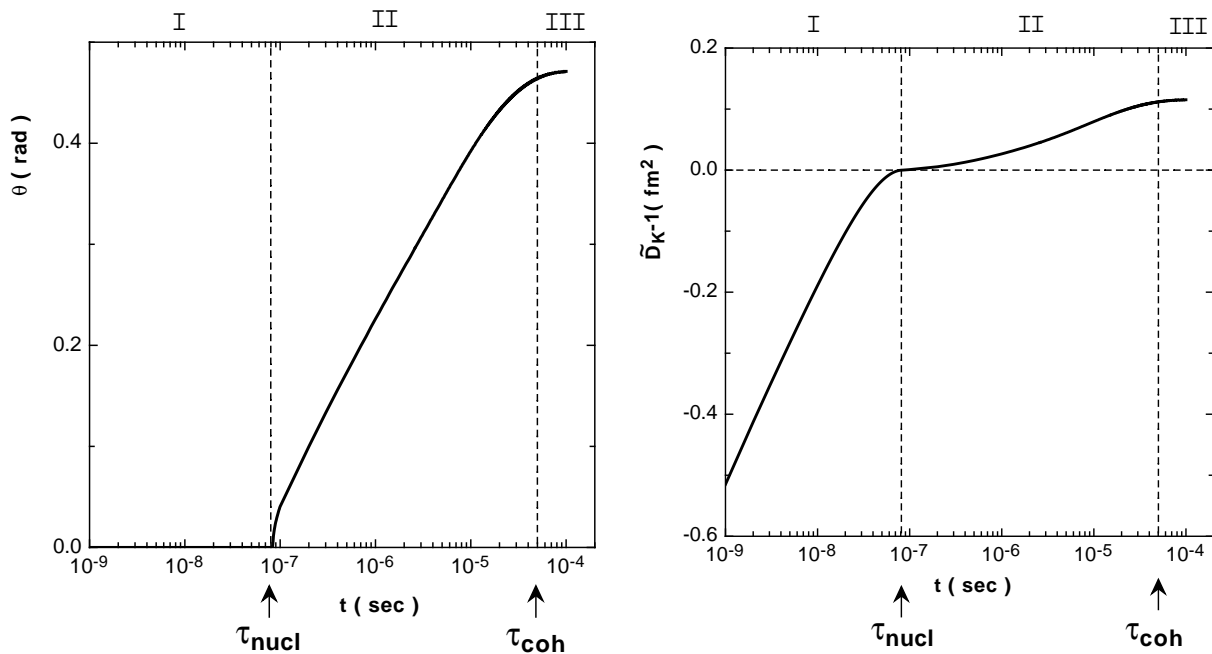


FIG. 1. (a) Chiral angle  $\theta$  and (b)  $\tilde{D}_K^{-1}$ , the negative of the expansion coefficient for the thermodynamic potential per unit volume  $\Omega/V$  with respect to the squared classical kaon field, as a function of time for the baryon number density  $n_B=0.55 \text{ fm}^{-3}$  and the temperature  $T=1.0 \times 10^{11} \text{ K}$ .

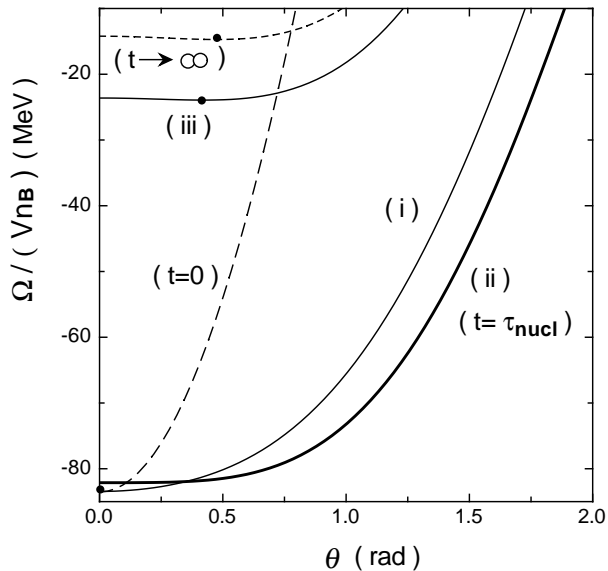


FIG. 2. Thermodynamic potential per particle  $\Omega/(Vn_B)$  as a function of  $\theta$  corresponding to the three cases (i)–(iii). The long-dashed and short-dashed lines correspond to the cases at  $t = 0$  and  $t \rightarrow \infty$ , respectively. The dots on the lines represent the locations of the minima of  $\Omega$ .



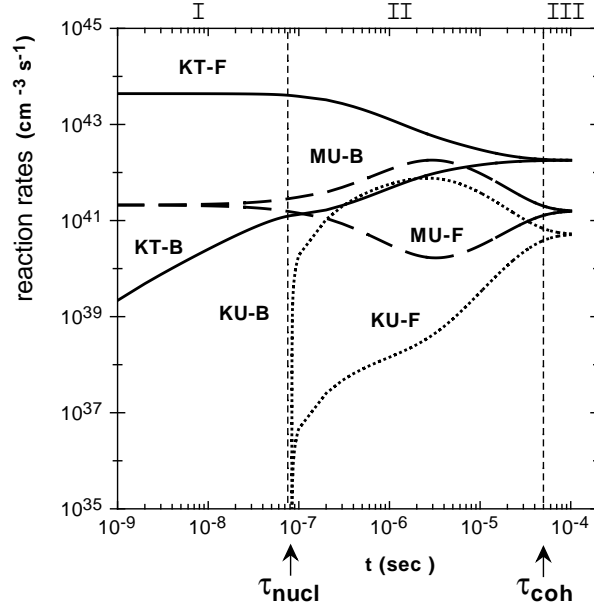


FIG. 3. Temporal behavior of the reaction rates for the weak reactions, KT, KU, and MU for  $n_B=0.55 \text{ fm}^{-3}$  and  $T = 1.0 \times 10^{11} \text{ K}$ .

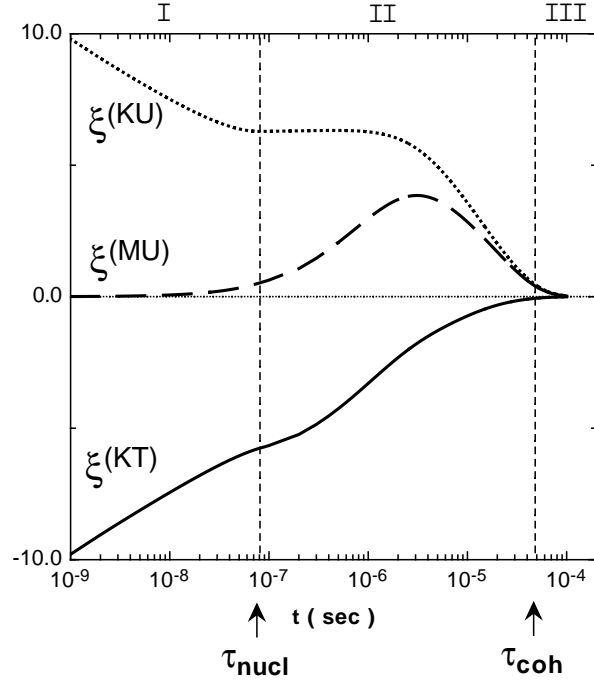


FIG. 4. Temporal behavior of the dimensionless parameters  $\xi^{(\alpha)}$  ( $\alpha = \text{KU, MU, KT}$ ) for  $n_B=0.55 \text{ fm}^{-3}$  and  $T = 1.0 \times 10^{11} \text{ K}$ .

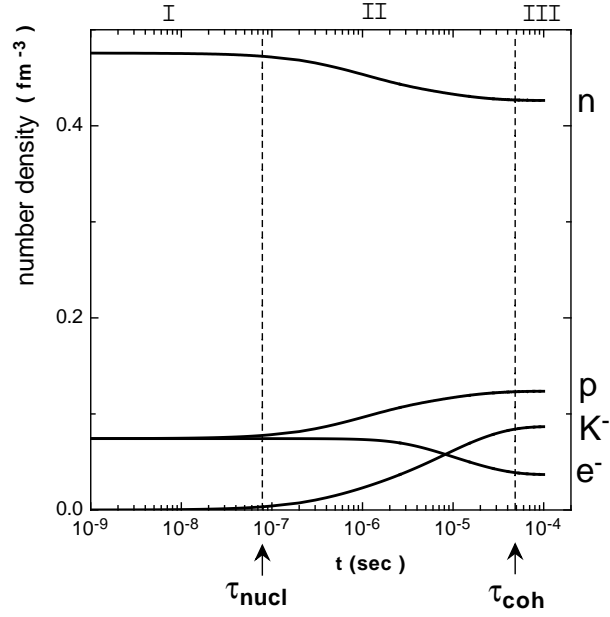


FIG. 5. Temporal behavior of the number densities of the chemical species.

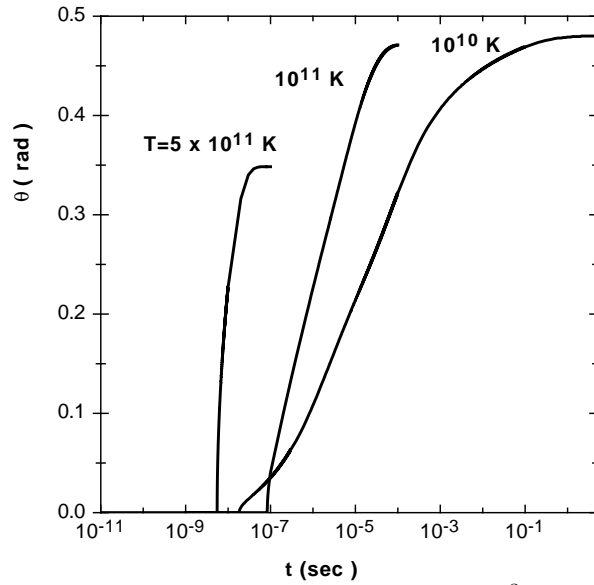


FIG. 6. Temporal behavior of the chiral angle  $\theta$  for  $n_B=0.55 \text{ fm}^{-3}$  and three different temperatures,  $T = 1.0 \times 10^{10} \text{ K}$ ,  $1.0 \times 10^{11} \text{ K}$ , and  $5.0 \times 10^{11} \text{ K}$ .

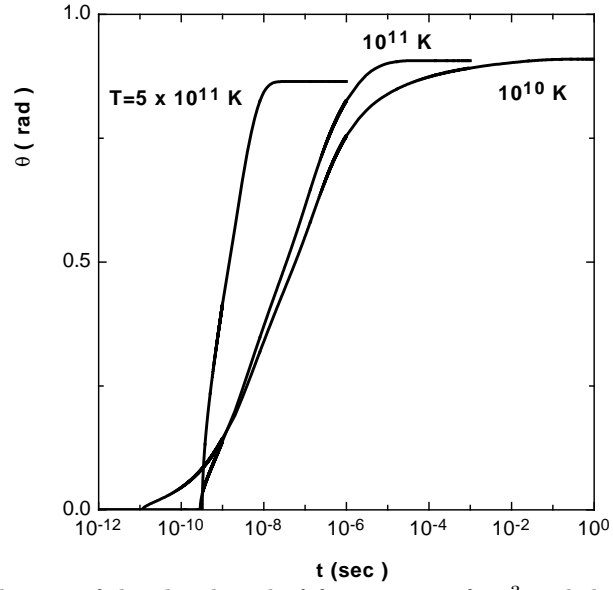


FIG. 7. Temporal behavior of the chiral angle  $\theta$  for  $n_B=0.70 \text{ fm}^{-3}$  and three different temperatures,  $T = 1.0 \times 10^{10} \text{ K}$ ,  $1.0 \times 10^{11} \text{ K}$ , and  $5.0 \times 10^{11} \text{ K}$ .